Available online at www.sciencedirect.com
ScienceDirect
Earth and Planetary Science Letters 257 (2007) 29–36
EPSL
www.elsevier.com/locate/epsl

Predicting trench and plate motion from the dynamics of a strong slab

Claudio Faccenna [a,*], Arnauld Heuret [b], Francesca Funiciello [a], Serge Lallemand [b], Thorsten W. Becker [c]

[a] Dipartimento Scienze Geologiche, Università Roma TRE, Roma, Italy
[b] UMR CNRS-UM2 5573, Lab. de Dynamique de la Lithosphere, Montpellier, France
[c] Department of Earth Sciences, University of Southern California, Los Angeles CA, USA

Received 12 July 2006; received in revised form 10 January 2007; accepted 6 February 2007
Available online 13 February 2007
Editor: R.D. Van der Hilst

Abstract

The motion of oceanic plates is commonly related to the subduction of cold and dense oceanic material into the mantle. These models predict plate velocities from subduction velocities but the trench motion is not directly included in the computation. Here, using a recent compilation of a global data set, we found that the motion of trenches (either advancing or retreating with respect to upper plates) scales with their corresponding subducting plates motion. Based on simple experimental tests, we found that subduction of strong slabs inside the upper mantle correctly predicts these kinematic relationships. We deduce that the motion of the trenches represent the surface manifestation of the resistance encountered by the subducting lithosphere to bend and penetrate within the upper mantle.

Keywords: subduction; oceanic plate; trench; laboratory experiments

1. Introduction

Plates bounded by subduction zones move faster than others, suggesting that slabs strongly determine plate motions. Two mechanisms have been proposed to explain the way slabs transmit their motion to the plates [1–3]. The first assumes that plates are pulled directly toward trenches by slabs [1,4], while the second assumes that plates are indirectly dragged by mantle circulation excited by the subducting lithosphere. Reasonable plate velocities can be obtained for both solutions when the amount of subducted material and slab coupling with the mantle is varied [2,5–8]. These calculations do not directly include the motion of the trenches in the computation of the subduction velocity. Previous models, however, revealed that trench motion is directly related to slab dynamics and to its ability to subduct into the mantle [9–17]. Following these results, we here analyze the motion trench as a proxy for the plate/slab system dynamics, thus representing the surface manifestation of the resistance of the subducting lithosphere to bend and penetrate into the upper mantle.

In the hot spot references frame, HS3-Nuvel 1A model [18], trenches either advance (53%) or retreat (47%) with respect to the upper plates at an average Vt

* Corresponding author. Tel.: +39 6 54888029; fax: +39 6 54888201.
E-mail address: faccenna@uniroma3.it (C. Faccenna).

0012-821X/$ - see front matter © 2007 Elsevier B.V. All rights reserved.
doi:10.1016/j.epsl.2007.02.016

rate ranging from −25 to 40 mm/yr, respectively [19] (Figs. 1 and 2). Except for Tonga (Fig. 2), advancing trenches are mainly distributed along the western side of the Pacific subduction zones where slabs are steeper ("Marianas" type of Uyeda and Kanamori [20]), whereas retreating trenches are distributed mainly on the eastern side where slabs are shallower ("Chilean" type of Uyeda and Kanamori [20]). Because of the upper plate motion, backarc extension is found mainly along the western side of the Pacific, whereas compression occurs along the eastern Pacific trenches. Plates move towards subduction zones with a broad spectrum of velocity Vp ranging from 4 to 11 cm/yr, representative of the eastern (Nazca, Cocos plate) and western (Pacific plate) side of the Pacific, respectively [18]. The relationships between the motion of the downgoing plates and related trenches are not fortuitous, as slow plates are attached to retreating trenches whereas faster plates are attached to advancing trenches (Fig. 2). This suggests that the motion of trenches represents a first order ingredient in plate–slab kinematics. This also indicates that the effective subduction velocity range Vs, resulting from the sum of trench and plate velocity (Fig. 2), is substantially narrower (63±23 mm/yr) than the trench and plate velocity itself (Fig. 2a). The kinematic relationship between trenches and subducting plates are confirmed, although less pronounced, by other hot-spot models [21,22], but flats down in the no-net-rotation reference frame.

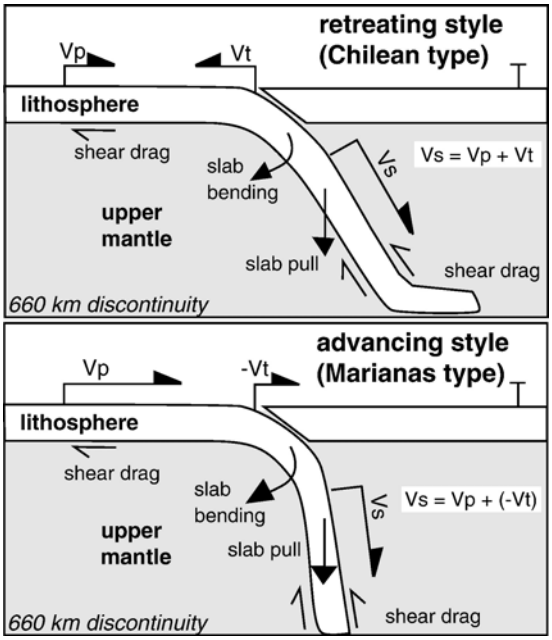

Fig. 1. Cartoon illustrating the advancing or retreating style of subduction. These two subduction styles, inspired by and resembling to the "Marianas" and the "Chilean" styles of Uyeda and Kanamori [20], cause a difference in the partitioning of the subduction velocity between trench and plate velocity. For a given subduction velocity, an advancing trench promotes faster plate velocity with respect to a retreating one. The two styles of subduction depend primary upon the force balancing between the slab pull and viscous dissipation due to the slab–mantle shear drag and to slab bending. Overriding plate motion is not considered in the model as a driving mechanism.

2. Laboratory experiments

Numerical and laboratory models have been focused on the subduction process and trench migration. Some of them investigate slab geometry as a function of imposed trench migration [23–26], while others analyzed the trench motion as the result of slab dynamics [15–18,27–32]. Following this second approach, we explored the significance of the kinematic relationships between trench and plate using simple laboratory tests. We modeled subduction using a thin (around 1 cm), large (around 20×40 cm^2), linearly viscous and dense plate of silicone putty sinking inside a large (0.8×0.8 m^2) tank filled with viscous glucose syrup. Silicone putty is a visco-elastic material that, at experimental strain rates, behaves only viscously as the experimental time-scale is higher than the Maxwell relaxation time (about 1 s). The upper mantle was modeled by glucose syrup, which is a Newtonian low-viscosity and high-density fluid. Experimental material, and similarity criteria are listed in Table 1 (see also [29]). The experiment were scaled to natural gravity fields respecting similarity criteria for stress and strain: The scale factor for length (*Lmodel*/*Lnature*) is $1.6\ 10^{-7}$ so that 1 cm in the experiment corresponds to 60 km. The scale density factor between the oceanic lithosphere and the upper mantle is 1.07 whereas the viscosity ratio between the slab and mantle is about 2000. Considering the imposed scale ratio for length, gravity, viscosity and density (Table 1), we calculate that 1 min in the model corresponds to about 3 Myr in nature. The model has been designed considering the following assumptions and simplifications: (1) viscous rheology; (2) no external forces; (3) passive convective mantle; (4) isothermal system; (5) the 660-km discontinuity is simulated by an impermeable barrier for the analyzed time scale. To isolate the role of the trench from other external contributions, we did not include the upper plate in our experiment: the role of an active pushing upper plate is described elsewhere [31].

Here, we present the result of 11 experiments performed to investigate how the plate–trench kinematic relationships depends upon experimental parameters such as width, viscosity, thickness, and density of the

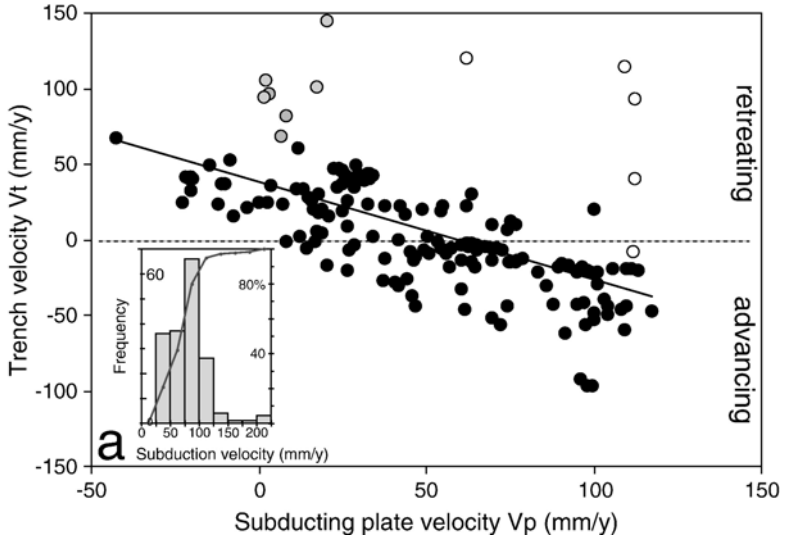

Fig. 2. Velocity field of the normal-to-trench component of subducting plate and trench velocity in the hot spot references frame (model HS3-NUVEL1A [18]). Data are extracted from 180 cross-sections of oceanic subduction "non-perturbed" by subduction of ridges or oceanic plateau, using a sampling step of 220 km covering nearly 36,000 km of trenches. Trench motion is calculated by subtracting the deformation velocity estimated by geodetic data of the backarc region from the upper plate velocity, assuming negligible erosion and accretion at trench (<10 mm/yr, [45]). Absolute velocities are defined as positive trenchwards. Advancing and retreating are negative and positive, respectively. The diagram illustrates that a fast retreating trench is generally related to slow subducting plate motion. The correlation coefficient of the linear regression is 0.60, which is increased to 0.74 if Tonga (white dot), New Hebrides and Luzon (grey dot) are excluded. In these regions, vigorous toroidal mantle circulation is active around slab edges producing a unique kinematic pattern [38–40]. Bottom left: (a) histogram of the normal to trench subduction velocity obtained adding the trench to the plate velocity.

plate. These experiments are part of a large experimental programme carried out by the Laboratory of Experimental Tectonics of the University of Roma TRE during the last six years to test the sensitivity of the modelling technique under a wider range of parameters and boundary conditions [15,16,29,31–33]. The model evolution is characterized by three stages: (i) after the initial, forced initiation, the slab progressively accelerates while sinking inside the mantle; (ii) the slab sharply decelerates during its interaction with the bottom of the tank and then (iii) reaches a steady-state configuration. This model evolution is in agreement to what has been found in previous simulations [11,12,14,16,26,29]. With varying experimental parameters (width, viscosity, thickness, and density of the plate, see Table 1 online material), the style of subduction during the steady-state configuration differs, assuming either an "advancing" or "retreating" trench style [29] (Fig. 3). The advancing trench style is characterized by a steeper slab and fast plate motion whereas the retreating trench style is characterized by a shallow dip slab and slow plate velocity. A linear regression describes the relationships between trench and plate velocity in the experiments, similarly to what observed in natural system (Fig. 3). The diagram also reveals that experimental trenches are not stationary but move away with respect to the deep anchored slab tip. This behavior is also probably enhanced by the presence of a deep impermeable barrier at 660 km depth equivalent. We also found that the subduction velocity Vs is higher in the "retreating" style compared to the "advancing" one, indicating that favourable subduction conditions, e.g. increasing the negative

Table 1
Laboratory and natural subduction reference parameters

Symbol (unit)	Parameters	Ref. nature	Ref. model
g (m s^{-2})	Gravitational acceleration	9.81	9.81
h (m)	Thickness oceanic lithosphere	80,000	0.012
H (m)	Thickness upper mantle	660,000	0.11
ρ_l (kg m^{-3})	Density oceanic lithosphere	3320	1482
ρ_m (kg m^{-3})	Density upper mantle	3220	1382
η_l (Pa s)	Viscosity oceanic lithosphere	10^{24}	10^5
η_m (Pa s)	Viscosity upper mantle	10^{21}	10^2
t^o (s)	Characteristic time	3.1×10^{13}	20

The characteristic time is derived from $(\Delta\rho\ gL)_{nature}/(\Delta\rho\ gL)_{model}$ $(\eta_{model}/\eta_{nature})$.

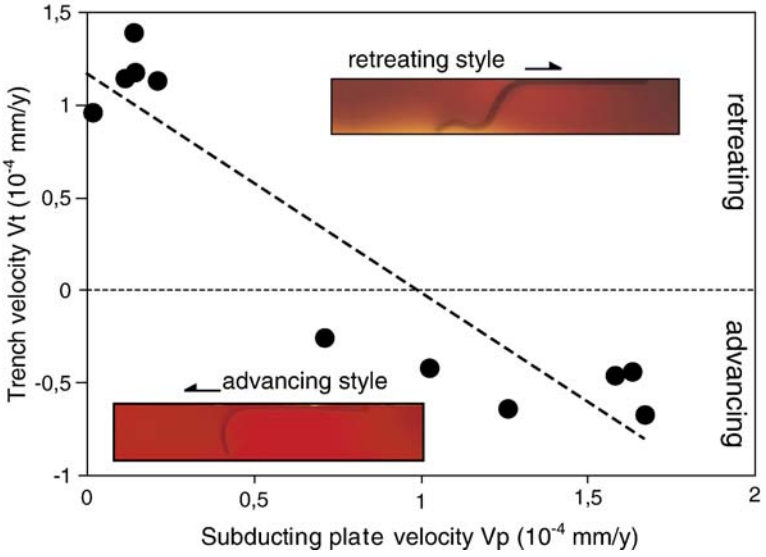

Fig. 3. Velocity field of the subducting plate and trench velocities in laboratory experiments. Linear regression coefficient is 0.93. Pictures show a snapshot of advancing and retreating styles of subduction experiments.

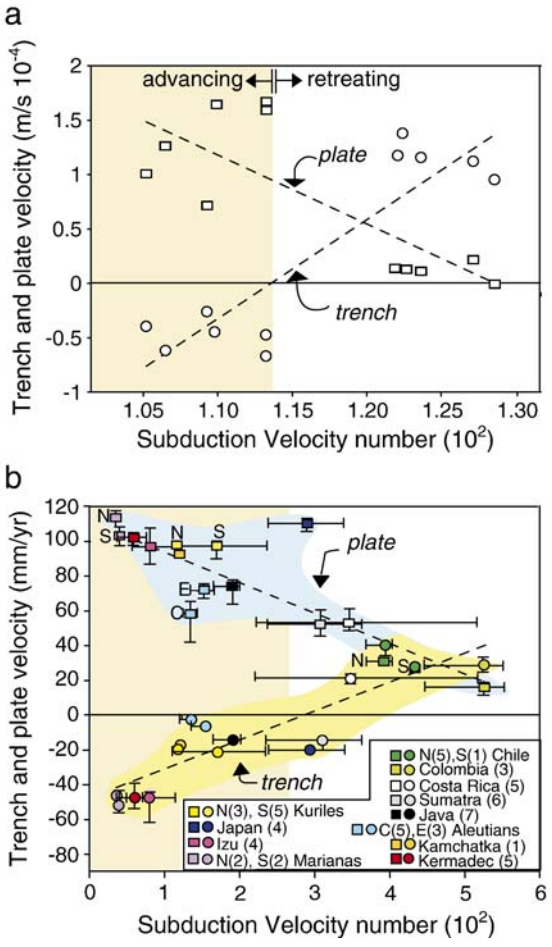

buoyancy of the plate, promote retreating trench migration and slab rollback. Therefore, the partitioning between trench and plate velocity is a function of the subduction velocity which, in turn, depends upon the dynamic equilibrium of the subduction system [29]. This force balance can be expressed as the ratio between the driving force, given by the negative buoyancy of the slab, and resisting forces, which are here mainly represented by two terms [29]. The first and larger one is related to viscous dissipation due to the bending of the slab. This term scales with the viscosity of the lithosphere (η_l) and the cube of the ratio between the plate thickness (h) and the radius of curvature (r) [15,34,35]. The second term, related to the resistance of the slab/plate system to penetrate and slide into the mantle, scales with the viscosity of the mantle (η_m) and the plate dimension (A) [34]. Following Conrad and Hager [34] and Bellahsen

Fig. 4. (a) Trench and plate velocity measured in the experiments versus velocity number. The regression coefficient R for trench and plate velocity is 0.89 and 0.79, respectively. (b) Averaged trench and plate velocity (component perpendicular to trench) for 16 main subduction zones (60 cross sections) versus subduction velocity number V. The regression coefficient R of the linear regression for plate and trench velocity is 0.85 and 0.88, respectively. Numbers near each subduction zone name indicate the number of cross-sections, letters the geographic portion of the subduction zones (N=North, S=South, E=East, C=Central). Note that natural and experimental velocity numbers differ by a constant related to the different boundary conditions [see also [29,34]].

et al. [29], the predicted subduction velocity (V') then scales as:

$$V' \approx \Delta\rho g h L/[2\eta_l(h/r)^3 + 3\eta_m A]. \quad (1)$$

Here, $\Delta\rho$ is the density contrast between the slab and the mantle, g is the gravitational acceleration, L is the slab length, A is the total surface of the slab–plate subjected to shear mantle drag equal to $(2(HW)^{1/2} + (Wl)^{1/2})/H$, being W the plate width, H the mantle thickness, and l the plate length. The predicted subduction velocity V' can be normalized by a characteristic velocity $V°=(\Delta\rho° g H° h°)/\eta_m°$ obtained for a Stokes sinker using reference parameters for a standard subduction system (Table 1), giving a dimensionless subduction velocity number V:

$$V = V'/V° = (hL/h°H°)[1/(2(\eta_l/\eta_m)(h/r)^3 + 3A)] \quad (2)$$

Fig. 4a shows that the subduction velocity number V predicts the style of subduction and the partitioning of the subduction velocity between plate and trench velocity. This relationship indicates that the style of subduction at a steady state depends upon the dynamical equilibrium between slab pull and the plate bending resistance plus mantle drag.

3. Predicting plate velocity for natural systems

In natural system, the laboratory-derived scaling rule can only be applied when the inherent simplicity of the experimental setting is taken into account. External contributions, such as motion of the overriding plate or interaction with other plates and slabs, is absent in this simple model, as is absent any kind of large-scale mantle flow. For this reason, we selected only the wider subduction zones excluding their lateral tips, where vigorous toroidal flow is found to be extremely active (i.e. Tonga, northern Kamchatka etc., [37–40]) and the small subduction zones (<2000 km), whose kinematics can be forced by background mantle flow. We also excluded oblique subduction (>45°) and subduction zones where physical parameters, such as slab dip or depth and radius of curvature, are poorly constrained (Ryukyu, Alaska). The remaining 60 cross-sections are representative of the following subduction zones: Java, Sumatra, Kermadec, Marianas, Izu-Bonin, Japan, Kuriles, Kamchatka, Aleutians, Costa Rica, Chile, Colombia (see Table 1 online material).

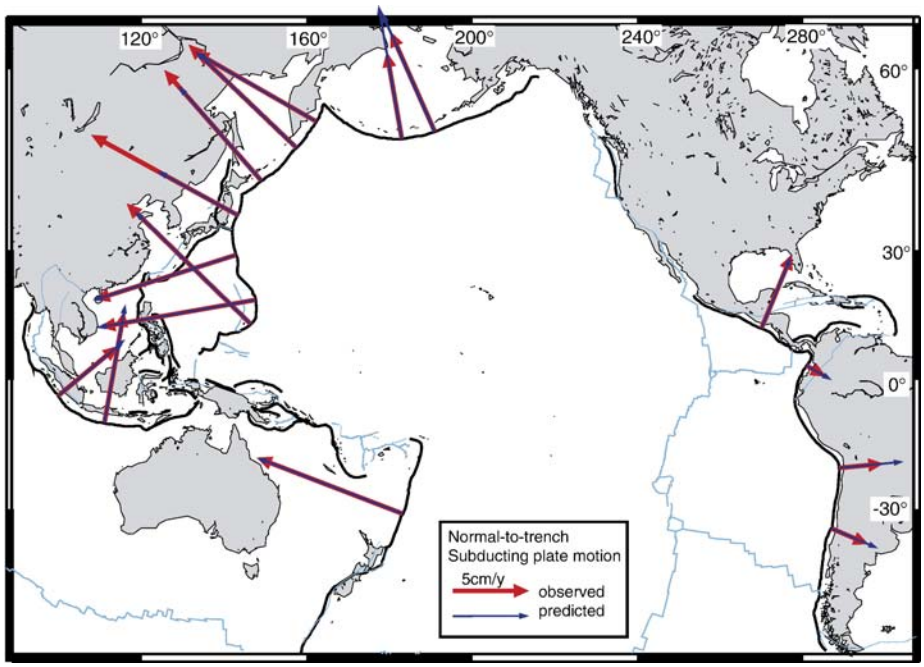

Fig. 5. Predicted versus observed normal-to-trench component of plate motion averaged over each subduction zone as shown in Fig. 4b. Mismatches are found systematically in oblique subduction regions system like the Aleutians, where normal to trench section slab parameters cannot be representative and along the cusps, mainly Japan, where the slab is anomalously shallow.

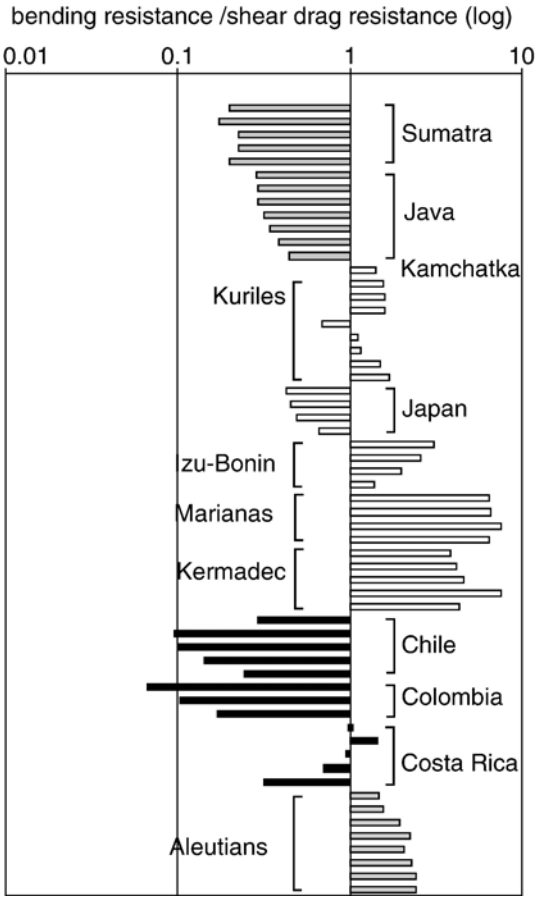

Fig. 6. Ratio between bending and shear drag forces calculated for the whole set of natural cross-sections. The absolute value of the two contributions should only be considered as indicative as scaling constants are not considered in the calculations [see also [29,34]].

The parameters of Eq. (2) for these subduction zones have been estimated using the following criteria. Slab length L is calculated by summing up the contribution related to the mean shallow dip (0–125 km) and to the mean deep dip (125 km–660 km depth) (see [19] for details). The length of the slab L does not include the slab segments that lie on top of, or pass through, the 660 km discontinuity, as it is supposed not to directly contribute to slab pull. Dips and radius of bending (r) were measured using Benioff zones from the EHB98 catalogue [19]. Tomographic images were used to estimate the dip when deep parts of slabs are aseismic. Uncertainties were estimated to be about ±2.5° for 2/3 of the cross-sections, and ±5° for the others. A is the plate/slab mantle interface, as defined above, with W as the trench length and l the trench–ridge distance. $H°$ is the upper mantle thickness, equal to 660 km. For plate thickness we tested two different models. In Mod.1 the plate thickness was set equal to $2(ka)^{1/2}$, with a being the age of the oceanic floor at trench (estimated from the digital grid of Müller et al. [41] averaging the subducting plate age on the first 10 km normal from trench) and k the thermal diffusivity. A variation of Mod.1 includes a threshold value of 100 km for lithosphere older than 80 Ma. In Mod.2, the plate thickness contributing to slab pull is averaged to 80 km, smoothing possible errors regarding the age and thermal structure of the subducted slab, whereas plate thickness in bending term is calculated using Mod.1 criterion.

Fig. 4b shows that the motion of plates and trenches is a linear function of the subduction velocity number, which in turn depends upon the radius of curvature, dips of the slab, length and width of the plate and plate thickness for Mod.2. There are similar distribution results for Mod.1, but with a lower regression coefficient value, due to the shift of Japan towards a higher value of the subduction velocity number (see below).

The Fig. 4b result is also illustrated on the Fig. 5 map, where the predicted components of plate velocities perpendicular to the trench are plotted over the observed ones. The predicted velocities fit the observed one with a mean error of ~17% carried on mainly by oblique segments (Aleutians) and by Japan (Table 2 online material). Three main implications follow from the success of our model. First, the negative buoyancy necessary to pull the plate is limited to the upper mantle portion of the slab. The slab's lower mantle portion, well imaged by global mantle tomography [10], appears to play a subordinate role in plate motions [cf. [3,7,36]] and may be sustained by the higher mantle viscosity there [e.g. [42,43]]. Second, the slab has to be about three orders of magnitude stronger than the upper mantle, to the point that its resistance to bend at trench is, on average, 1.7 times larger than the one offered by the mantle–slab shear drag (Fig. 6). This is a similar ratio to what was proposed using different approaches [34,36]. Indeed, experimental tests show that under these conditions [cf. [29,31]], small variations of lithosphere–plate properties, such as age, crustal thickness or plate width and length, cause a switch of subduction styles, from the "Marianas"- to the "Chilean"-type [20], producing changes of plate and trench speed, and consequently, of the backarc tectonic regime. Such alternations of compressional and extensional episodes are recorded in backarc regions. Third, the Uyeda and Kanamori's [20] dichotomy of the subduction styles on the Pacific sides is here explained by local slab dynamics, which in turn produce the difference between the Nazca and Pacific plate speeds. Interactions of slabs with the deep mantle thus appear to contribute significantly to the net rotation of the lithosphere with respect to the lower mantle.

Our model fails in reproducing the kinematics of some narrow slabs (e.g. Sandwich, Caribbean, Cascade, New Hebrides) or portions of large subduction zones, notably Tonga or Japan. This is due to the fact that we cannot account for 3D complexities, such as the presence of lateral, out-of-plane toroidal flow that is thought to be particularly efficient in producing the extremely fast retreating rate recorded for the Tonga [37] and creating the Japan cusp-like structure, dominated by an anomalous shallow slab dip (29°, [19,21,44]). With respect to previous analysis [e.g. [2,3,6,7]], our prediction is also limited to the motion of the subducting plates. Despite these limitations, this model is able to explain the migration of the trench and the motion of the large plate in a unique coherent system. Plates are controlled by slabs descending into the upper mantle, dissipating energy while bending at the trench and penetrating into the upper mantle. Slabs are strong entities, which preserve part of their lithospheric integrity and are poorly coupled to the upper mantle, partitioning their motion between trenches and plates and giving rise to the variety of "plate tectonic" behavior along convergent margins.

Acknowledgements

N. Bellahsen performed some of the experiments presented here at the Laboratory of Experimental Tectonics of Roma TRE University. The idea expressed here benefits from discussion with C. Conrad, C. Doglioni, and L. Husson. We are grateful for the review by S. King, the anonymous referee, R. van der Hilst and to Cynthia Rockwell for English editing.

Appendix A. Supplementary data

Supplementary data associated with this article can be found, in the online version, at doi:10.1016/j.epsl.2007.02.016.

References

[1] D. Forsyth, S. Uyeda, On the relative importance of the driving forces of plate motion, Geophys. J. R. Astron. Soc. 43 (1975) 163–200.
[2] T.W. Becker, R.J. O'Connell, Predicting plate velocities with mantle circulation models, Geochem. Geophys. Geosyst. 2 (2001), 10.1029/2001GC000171.
[3] C.P. Conrad, C. Lithgow-Bertelloni, How mantle slabs drive plate tectonics, Science 298 (2002) 207–209.
[4] W. Spence, Slab pull and the seismotectonics of subduction lithosphere, Rev. Geophys. 25 (1987) 55–69.
[5] D.L. Turcotte, E.R. Oxburgh, Finite amplitude convective cells and continental drifts, J. Fluid Mech. 28 (1967) 29–42.
[6] Y. Ricard, C. Vigny, Mantle dynamics with induced plate tectonics, J. Geophys. Res. 94 (1989) 17,543–17,560.
[7] C. Lithgow-Bertelloni, M.A. Richards, The dynamics of Cenozoic and Mesozoic plate motions, Rev. Geophys. 36 (1998) 27–78.
[8] C.P. Conrad, C. Lithgow-Bertelloni, Temporal evolution of plate driving forces: the importance of "slab pull" and "slab suction" as forces that drive plate motions, J. Geophys. Res. 109 (2004) B01407, doi:10.1029/2004JB002991.
[9] R. Van der Hilst, T. Seno, Effects of relative plate motion on the deep structure and penetration depth of slabs below the Izu-Bonin and Mariana island arcs, Earth Planet. Sci. Lett. 120 (1993) 395–407.
[10] R. Van der Hilst, R. Engdahl, W. Spakman, G. Nolet, Tomographic imaging of subducted lithosphere below northwest Pacific island arcs, Nature 353 (1991) 37–43.
[11] M. Gurnis, B.H. Hager, Controls of the structure of subducted slabs, Nature 335 (1988) 317–321.
[12] S. Zongh, M. Gurnis, Mantle convection with plates and mobile, faulted margins, Science 266 (1995) 838–843.
[13] J. Chen, S.D. King, The influence of temperature and depth dependent viscosity on geoid and topography profiles from models of mantle convection, Phys. Earth Planet. Inter. 106 (1998) 75–91.
[14] J.J. Ita, S.D. King, The influence of thermodynamic formulation on simulations of subduction zone geometry and history, Geophys. Res. Lett. 125 (1998) 1463–1466.
[15] C. Faccenna, F. Funiciello, D. Giardini, F.P. Lucente, Episodic backarc extension during restricted mantle convection in the Central Mediterranean, Earth Planet. Sci. Lett. 187 (2001) 105–116.
[16] F. Funiciello, C. Faccenna, D. Giardini, K. Regenauer-Lieb, Dynamics of retreating slabs (part 2): insights from 3D laboratory experiments, J. Geophys. Res. 108B4 (2003).
[17] L. Royden, H. Leigh, L. Husson, Laurent Trench motion, slab geometry and viscous stresses in subduction systems. Geophys. J. Int. 167 (2), (2006) 881–905, doi: 10.1111/ j.1365-246X.2006.03079. x.
[18] A.E. Gripp, R.G. Gordon, Young tracks of hot spot and current plate velocities, Geophys. J. Int. 150 (2002) 321–361.
[19] A. Heuret, S. Lallemand, Plate motions, slab dynamics and back-arc deformation, Phys. Earth Planet. Inter. 1491-2 (2005) 31–51.
[20] S. Uyeda, H. Kanamori, Back-arc opening and the mode of subduction, J. Geophys. Res. 84 (1979) 1049–1061.
[21] R.D. Jarrard, Relations among subduction parameters, Rev. Geophys. 24 (1986) 217–284.
[22] R.G. Gordon, D.M. Jurdy, Cenozoic global plate motion, J. Geophys. 91 (1986) 12,389–12,406.
[23] R.W. Griffiths, R.I. Hackney, R.D. van der Hilst, A laboratory investigation of effects of trench migration on the descent of subducted slabs, Earth Planet. Sci. Lett. 133 (1995) 1–17.
[24] L. Guillou-Frottier, J. Buttles, P. Olson, Laboratory experiments on structure of subducted lithosphere, Earth Planet. Sci. Lett. 133 (1995) 19–34.
[25] U.R. Christensen, The influence of trench migration on slab penetration into the lower mantle, Earth Planet. Sci. Lett. 10 (1996) 27–39.
[26] S.D. King, Subduction: observations and geodynamic models, Phys. Earth Planet. Inter. 127 (2001) 9–24.
[27] C. Kincaid, P. Olson, An experimental study of subduction and slab migration, J. Geophys. Res. 92 (1987) 13,832–13,840.

[28] A. Enns, T.W. Becker, H. Schmeling, The dynamics of subduction and trench migration for viscosity stratification, Geophys. J. Int. 160 (2) (2005) 761–775, doi:10.1111/ j.1365 246 X.2005.02519.x.
[29] N. Bellahsen, C. Faccenna, F. Funiciello, Dynamics of subduction and plate motion in laboratory experiments: insights into the "plate tectonics" behavior of the Earth, J. Geophys. Res. 110B01401 (2005), doi:10.1029/2004JB002999.
[30] W.P. Schellart, Quantifying the net slab pull force as a driving mechanism for plate tectonics, Geophys. Res. Lett. 31L07611 (2004).
[31] A. Heuret, F. Funciello, C. Faccenna, S. Lallemand, Plate kinematics, slab shape and back-arc stress: a comparison between laboratory models and current subduction zones, Earth Planet. Sci. Lett. (in press), doi:10.1016/j.epsl.2007.02.004.
[32] F. Funiciello, C. Faccenna, D. Giardini, Role of lateral mantle flow in the evolution of subduction system: insights from 3-D laboratory experiments, Geophys. J. Int. 157 (2004) 1393–1406.
[33] F. Funiciello, M. Moroni, C. Piromallo, C. Faccenna, A. Cenedese, H.A. Bui, Mapping mantle flow during retreating subduction: laboratory models analyzed by feature tracking, J. Geophys. Res. 111 (B3) (2006), doi:10.1029/2005JB003792.
[34] C.P. Conrad, B.H. Hager, Effects of plate bending and fault strength at subduction zones on plate dynamics, J. Geophys. Res. 104 (1999) 17551–17571.
[35] D.L. Turcotte, G. Schubert, Geodynamics Application of Continuum Physics to Geological Problems, John Wiley and Sons, New York, 1982 450 pp.
[36] B.A. Buffett, D.B. Rowley, Plate bending at subduction zones: consequences for the direction of plate motions, Earth Planet. Sci. Lett. 245 (2006) 359–364.
[37] M. Bevis, F.W. Taylor, B.E. Schutz, J. Recy, B.L. Isacks, S. Helu, R. Singh, E. Kendrick, J. Stowell, B. Taylor, S. Calmant, Geodetic observations of very rapid convergence and back-arc extension at the Tonga Arc, Nature 3746519 (1995) 249–251.
[38] G.P. Smith, D.A. Wiens, K.M. Fischer, L.M. Dorman, S.C. Webb, J.A. Hildebrand, A complex pattern of mantle flow in the Lau backarc, Science 292 (2001) 713–716.
[39] D. Bercovici, Y. Ricard, M.A. Richards, The relation between mantle dynamics and plate tectonics: a primer, The History and Dynamics of Global Plate Motions, in: M.A. Richards, R. Gordon, R. Van der Hilst (Eds.), AGU Geophysical Monograph, vol. 21, 2000, pp. 5–46.
[40] C. Piromallo, T.W. Becker, F. Funiciello, C. Faccenna, Three-dimensional instantaneous mantle flow induced by subduction, Geophys. Res. Lett. 338 (2006) L08304, doi:10.1029/2005GL025390.
[41] R.D. Muller, W.R. Roest, J.Y. Royer, L.M. Gahagan, J.G. Sclater, Digital isochrons of the world's ocean floor, J. Geophys. Res.-Solid Earth 102B2 (1997) 3211–3214.
[42] B.H. Hager, Subducted slab and the geoid: constraints on mantle rheology and flow, J. Geophys. Res. 89 (1984) 6003–6015.
[43] J.X. Mitrovica, A.M. Forte, Radial profile of mantle viscosity: results from the joint inversion of convection and postglacial rebound observables, J. Geophys. Res.-Solid Earth 102B2 (1997) 2751–2769.
[44] C. Cruciani, E. Carminati, C. Doglioni, Slab dip vs. lithosphere age: no direct function, Earth Planet. Sci. Lett. 238 (2005) 298–310.
[45] S. Lallemand, High rates of arc consumption by subduction processes; some consequences, Geology 23 (1995) 551–554.